ACS APPLIED MATERIALS & INTERFACES

Letter

www.acsami.org

Salt-Responsive Self-Assembly of Luminescent Hydrogel with Intrinsic Gelation-Enhanced Emission

Chunqiu Zhang,[†,‡] Chang Liu,[†,‡] Xiangdong Xue,[†] Xu Zhang,[†] Shuaidong Huo,[†] Yonggang Jiang,[†] Wei-Qiang Chen,[§] Guozhang Zou,*[,†] and Xing-Jie Liang*[,†]

[†]CAS Key Laboratory for Biological Effects of Nanomaterials & Nanosafety, National Center for Nanoscience and Technology, No. 11 Beiyitiao, Zhongguancun, Beijing 100190, China

[§]Institute of Modern Physics, Chinese Academy of Sciences, Lanzhou 730000, China

Supporting Information

ABSTRACT: Tetraphenylethylene (TPE), an archetypal luminogen with aggregation-induced emission (AIE), was grafted to a salt-responsive peptide to yield a yet luminescent hydrogelator. After testing different parameters, we found that only in the presence of salt rather than temperature, pH, and solvent, did the monodisperse hydrogelators self-assemble into a hydrogel network with bright emission turned on. The induced luminescence was a dynamic change and enabled real time monitoring of hydrogel formation. Grating AIE molecules to stimuli-responsive peptides is a promising approach for the development of self-revealing soft materials for biological applications.

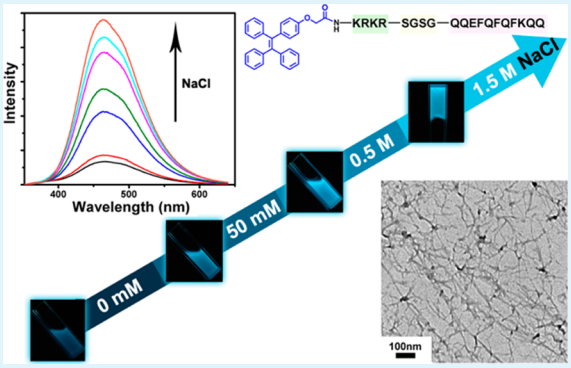

KEYWORDS: *salt-responsive, luminescent hydrogel, tetraphenylethylene (TPE), aggregation-induced emission (AIE), gelation-enhanced emission*

INTRODUCTION

Self-assembled molecular hydrogels have emerged as a new class of soft materials because of their great potential for drug delivery,[1−4] tissue engineering[5−9] and biosensor,[10,11] etc. In particular, luminescent hydrogels have gained considerable interest because of their advanced applications for fluorescence probes and biosensors.[12,13] However, most traditional π-conjugated luminescent molecules suffer from emission quenching in the condensed phase although they emit efficiently in solution as individual molecules. The strong intermolecular interactions that lead to self-assembled structures generally consume the excited state energy and thus debilitate the light emission of the hydrogels. Therefore, using traditional luminescent molecules to fabricate the luminescent hydrogel becomes a complex task and, in most cases, is a dilemma. In addition, using traditional fluorescent dyes to dope hydrogel and make it luminescent is rather a "static" approach and the fluorescence is always on. It is difficult to realize a "dynamic" visualization applied in tissue engineering and biosensor. Thus, to find solutions and develop tailored π-conjugated hydrogelators with efficient emissions in the aggregated state and stimulus-responding fluorescence is of great interest.

Herein, we designed the first example of salt-responsive peptide hydrogelator (TPE-Q19 in Figure 1) to form a luminescent hydrogel with enhanced emission upon gelation. The designed structure of the amphiphilic peptide hydrogelator has two segments for different functions, respectively. The tetraphenylethylene (TPE) was chosen as the luminogenic agent. TPE is an archetypal luminogen with intriguing aggregation induced emission (AIE), the phenomenon of which was first observed by Tang and co-workers in 2001.[14] TPE is almost nonfluorescent in solution but emits efficiently when aggregated into nanoparticles in a poor solvent or fabricated as a film in the solid state.[15−20] Because of its simple molecular structure, through facile chemical modification, many functional TPE-based materials have been developed and applied as fluorescent chemosensors,[21] bioprobes,[22,23] opto-electronic materials,[24] etc. The AIE phenomenon gives us a hint to resolve the dilemma of traditional fluorescent dyes. The second segment, peptide Q19, was derived from a reported peptide Q11 (Ac-QQKFQFQFEQQ-Am).[25−28] As with other previously reported short fibrillizing peptides,[29−31] β-hairpins,[32,33] peptide-amphiphiles,[34−36] and peptide derivatives,[37] peptide Q11 is able to self-assemble into a β-sheet fibrillar structure in salt-containing aqueous environments and then entangle to form a gel network. It has been found to be minimally immunogenic[38] and its salt sensitivity has also been utilized to develop materials that rapidly gel in response to other events, such as temperature or near-infrared light

Received: November 5, 2013
Accepted: December 29, 2013
Published: December 29, 2013

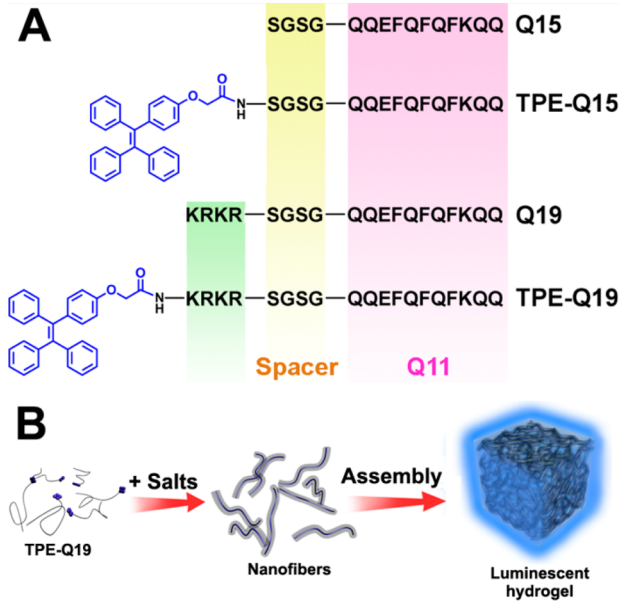

Figure 1. (A) Chemical structures of peptides used for molecular hydrogelations and (B) schematic illustration of the formulation of luminescent hydrogel by TPE-Q19.

exposure.[25,39] Thus, we opted to design peptide Q19 capped with TPE molecular as hydrogelator to form a salt-responsive luminescent hydrogel with gelation enhanced emission.

RESULTS AND DISCUSSION

To synthesize the luminescent hydrogelator, carboxylated tetraphenylethylene (TPE-COOH) was synthesized (see the Supporting Information, Figure S1) and characterized by ^{1}H NMR spectrum and ESI-MS (see the Supporting Information, Figure S2). Then, the designed peptide derivatives (Figure 1) could be obtained easily by solid phase peptide synthesis (SPPS). After synthesis by SPPS, purification by reverse phase HPLC and molecular weight determination by MALDI-TOF-MS (see the Supporting Information, Figure S3–S6), we tested the gelation ability by adding a measured amount of NaCl solution to peptide derivatives solution. We observed that Q15, Q19 ,and TPE-Q19 could form molecular hydrogels upon adding NaCl solution, whereas TPE-Q15 changed into precipitates even in pure water (see the Supporting Information, Figure S7). It seemed that introduction of the four hydrophilic amino acids (KRKR) between TPE and Q15 was very important for increasing the water-solubility of TPE and disrupting the precipitation. The minimum gelation concentration (MGC) was 0.3 wt % for both TPE-Q19 and Q15, much lower than that of Q19 (1.5 wt %). The results indicated that the incorporation of KRKR into N-terminal of Q15 inhibited the gelation of peptide Q19, while the incorporation of TPE to Q19 facilitated the formation of hydrogel. Thus, we chose TPE-Q19 as hydrogelator to fabricate the luminescent hydrogel. In addition, we also investigated the effect of other parameters on the gelation of TPE-Q19 (0.5 wt %), such as temperature (from 20°C to 80 °C) (see the Supporting Information, Figure S8), pH (from 1 to 14) (see the Supporting Information, Figure S9) and solvent (tetrahydrofuran and methanol) (see the Supporting Information, Figure S10), and found that these parameters showed no effect, so the gelation was primarily a salt-induced process.

As a proof-of-concept study, the gelation process and evolution of fluorescence emission spectra of TPE-Q19 (0.5 wt %) coupled with the increase in salt concentration were monitored. As shown in Figure 2A, the originally light-blue-colored solution gradually turned to bright-blue-colored gel under UV light when the concentration of NaCl increased to 1.50 M. As a result, we found that the fluorescence intensity at 466 nm corresponding to the emission from TPE gradually increased upon increasing the NaCl concentration (Figure 2B). When the concentration of NaCl reached to 1.50 M, the fluorescence intensity of TPE was nearly 8-fold stronger than in pure water solution (Figure 2C). To further confirm that the degree of gelation was determined by the salt concentration, we monitored gelation process of TPE-Q19 (0.5 wt %) incubated

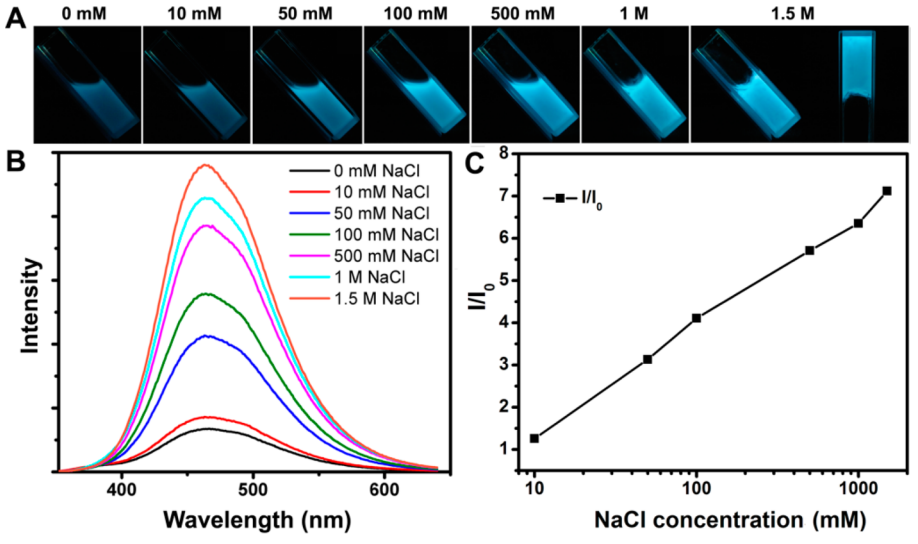

Figure 2. (A) Fluorescence images of the progressive gelation of TPE-Q19 (0.5 wt %) incubated with different concentrations of NaCl (0–1.5 M) under a 365 nm UV lamp. (B) Fluorescence spectra of TPE-Q19 (0.5 wt %) incubated with different concentrations of NaCl (0 to 1.5 M) (λ_{ex} = 330 nm). (C) Plot of fluorescence intensity (I) of TPE-Q19 (0.5 wt %) at 466 nm versus NaCl concentration (10 mM to 1.5 M), I_0 = fluorescence intensity of TPE-Q19 in pure water solution (λ_{ex} = 330 nm).

dx.doi.org/10.1021/am4049354 | ACS Appl. Mater. Interfaces 2014, 6, 757–762

with NaCl of different concentrations (see the Supporting Information, Figure S11A). The results showed that in the presence of NaCl with concentrations ranging from 0 mM to 500 mM, TPE-Q19 (0.5 wt %) didn't form hydrogels after 10 min, even 1 h. However, when the concentration of NaCl increased to 1 and 1.5 M, TPE-Q19 formed hydrogels within 10 min. Also, we investigated the time course of luminescence varied in the process of hydrogel formation. We incubated TPE-Q19 (0.5 wt %) with NaCl (1 M) for 10 min and checked the fluorescence every minute or two and found that the FL increased rapidly in the first minute, then slowly increased and began to level off at 10 min (see the Supporting Information, Figure S11B, C). This phenomenon of emission enhancement upon increasing the NaCl concentration might be ascribed to two different mechanisms. One is that TPE was not directly involved in the formation of nanostructures, but existed as individually exposed moieties in the hydrogel, whereas the gelation increased the viscosity of the surroundings, which would influence the intramolecular rotation (IMR) of the peripheral phenyl rings and ultimately lead to enhanced emission of TPE. The other mechanism is that TPE was involved in the formation of nanostructures and encapsulated into the inner of the structure. The entrapment of TPE molecules would restrict the IMR of peripheral phenyl rings and ultimately lead to enhanced emission of TPE. To explore the exact mechanism, we tested the fluorescence intensity changes in solution to eliminate the influence of increased viscosity. Surprisingly, turn-on fluorescence was observed when the TPE-Q19 concentration was only 100 μM (0.027 wt %) in dilute solution, which is much lower than MGC (Figure 3A, B). Under this condition where the concentration was below the MGC and no gelation took place, the enhanced emission of TPE could be attributed only to the formation of nanostructures rather than increased viscosity from gelation. Furthermore, the emission of the TPE-conjugated peptide-based hydrogel and TPE-COOH aggregating in water both showed a broad emission peak centered at 466 nm and this peak is corresponding to the fluorescence of TPE in aggregated state (see the Supporting Information, Figure S12). To further confirm the TPE molecules of hydrogelators were in aggregated state, circular dichroism (CD) spectra was investigated. As shown in Figure 3C, CD spectra of dilute solutions of TPE-Q19 (100 μM, 0.027 wt %) in pure water represented a conformation typical for unordered peptide. However, increasing NaCl concentration in TPE-Q19 solution caused a gradual change of the CD signal, with the appearance of a negative peak near 230 nm, indicative of unique aromatic $\pi-\pi$ interactions,[40] which can only be ascribed to the interactions among the TPE molecules. These results confirmed that the TPE moiety in TPE-Q19 was directly involved in the formation of the nanostructure.

It is interesting that the emission of TPE-Q19 was salt-responsive, whereas the fluorescence intensity of TPE-COOH aggregated in water solution was only slightly affected by the NaCl concentration (Figure 3D, E). Comparing their molecular structure, the only difference between them is the peptide segment Q19, which is salt-responsive. To explain this phenomenon, we then investigated the emission spectra of the benzathiole dye thioflavine T (ThT), which is a potent fluorescent marker of amyloid fibrils,[41] to understand relationship between the fluorescence change and the peptide conformation change of TPE-Q19. The enhanced emission of ThT incubated with TPE-Q19 (100 μM, 0.027 wt %) in the

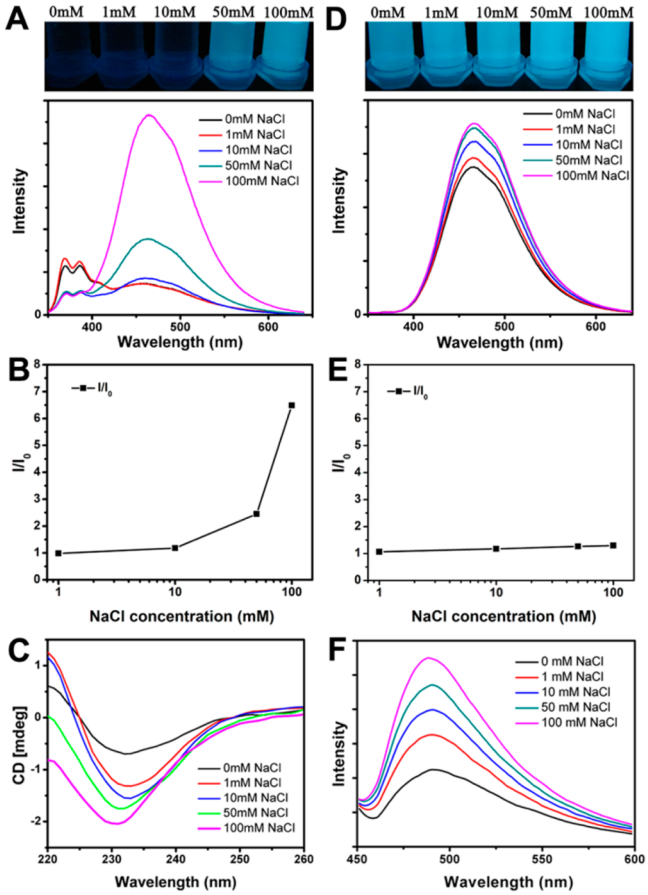

Figure 3. Fluorescence images and emission spectra of (A) TPE-Q19 dilute solution (100 μM, 0.027 wt %) and (D) TPE-COOH aggregated in solution (100 μM) mixed with different concentrations of NaCl (0 to 100 mM). Plot of fluorescence intensity (I) of (B) TPE-Q19 (100 μM, 0.027 wt %) and (E) TPE-COOH (100 μM) at 466 nm versus NaCl concentration (0−100 mM), I_0 = fluorescence intensity of TPE-Q19 or TPE-COOH in pure water solution (λ_{ex} = 330 nm). (C) Circular dichroism of TPE-Q19 in a dilute solution (100 μM, 0.027 wt %) with added NaCl (0−100 mM). (F) Fluorescence spectra of thioflavin-T in presence of TPE-Q19 peptide (100 μM, 0.027 wt %) under different NaCl concentration (0−100 mM) (λ_{ex} = 440 nm).

presence of increasing NaCl concentration confirmed the formation of β-sheet conformation (Figure 3F). The results demonstrated that conjugation of TPE to Q19 did not affect the Q11 section to form the β-sheet fibrillar structure, while in response to the increment of NaCl concentration, the emission of TPE was enhanced corresponding to the salt-induced aggregation of the peptide. Thus, we hypothesized that the Q11 section self-assembled into β-sheet amyloid fibrillar structure at the presence of salt and TPE molecules were sequestered in the interior of the nanofibers because of their hydrophobicity. The narrow space inside the nanofibers restricted the intramolecular rotation of TPE molecules, which ultimately led to the enhanced emission of TPE.

The mechanical property of the resulting luminescent gel containing 0.5 wt % of gelator was characterized by rheology. The aqueous solution containing gelator was directly transferred to the rheometer and then NaCl solution was equably added into the gelator solution with the final concentration of 1 M. After 10 min incubation, stable hydrogel was obtained. We then determined the linear viscoelastic region (LVR) (Figure

dx.doi.org/10.1021/am4049354 | ACS Appl. Mater. Interfaces 2014, 6, 757−762

4A) and performed a dynamic frequency sweep (Figure 4B). In the linear viscoelastic region, the value of dynamic storage

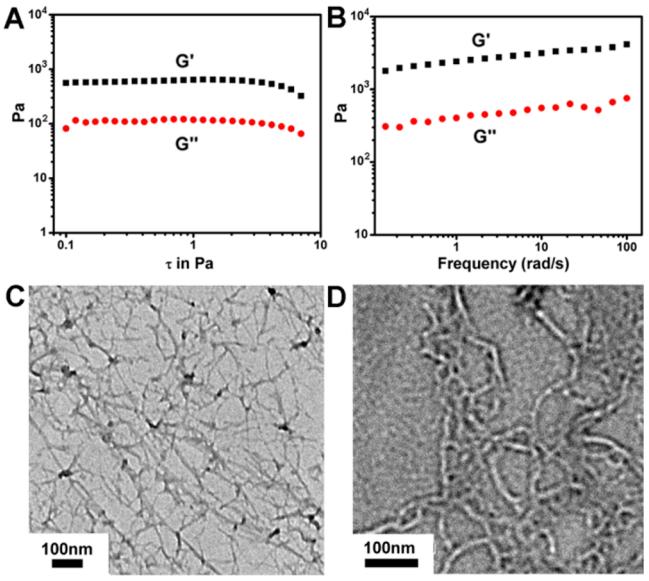

Figure 4. (A) Dynamic storage modulus (G') and loss modulus (G'') versus strain for TPE-Q19 hydrogel at 0.5 wt % concentration. (B) Frequency dependence of dynamic storage modulus (G') and loss modulus (G'') of TPE-Q19 hydrogel. Transmission electron microscopy (TEM) images of TPE-Q19 gel at (C) 0.5 wt % concentration and (D) Q19 gel at 1.5 wt % concentration.

moduli (G') of TPE-Q19 hydrogel was larger than that of its corresponding dynamic loss moduli (G''), suggesting the formation of a typical soft solidlike gel-phase material. The gel exhibited a G' value between 1000 and 10 000 Pa, indicating that the sample was of good mechanically strength. Mechanical strength of the hydrogel increased probably because of the hydrophobic interactions induced by the TPE molecules. Each gelator molecular containes a large hydrophobic TPE group, which has a very rigid structure. The interactions of gelators gave the gel excellent mechanical properties.

The morphology of TPE-Q19 and Q19 hydrogels was examined after gelation. The self-assembled structures in gels were characterized by transmission electron microscopy (TEM). As shown in images C and D in Figure 4, networks of nanofibers were observed in both hydrogels. The fibers in both gels entangled with each other to form the 3D network. In addition, the morphology of the progressive gelation of TPE-Q19 incubated with different concentrations of NaCl (from 0 to 1 M) was also examined by scanning electron microscope (SEM) (see the Supporting Information, Figure S13). The results showed that, with the increase of NaCl concentration, the formation of fiber and fiber network was gradually accumulating. On the other hand, we also found that TPE-Q19 gelators (100 μM, 0.027 wt %) were dark in water solution but turned to highly emissive when adding NaCl to this solution, demonstrating TPE-Q19 could also self-assemble to form aggregate at concentrations below the MGC. Thus, the nanostructure of TPE-Q19 in dilute solution (100 μM, 0.027 wt % in 100 mM NaCl) was investigated and found forming similar nanofibers of the hydrogel but much less entangled (see the Supporting Information Figure S14A). As control, the morphology of TPE-COOH aggregated in water was spherical in shape, with diameter about 100 nm (see the Supporting Information, Figure S14B).

Biodegradable luminescent hydrogels that allow 3D encapsulation of cells are important scaffolds to modulate cellular microenvironments with temporal and spatial resolution in the field of tissue engineering. Thus, we detected the biodegradable property of TPE-Q19 hydrogel for the potential application for tissue engineering. Because the sequence of peptide Q19 is rich in arginine and lysine residues, which are restriction sites by trypsin, we decided to test the biodegradable capability by enzymatic hydrolysis. As we expected, after incubated with 0.025% trypsin for 12h, TPE-Q19 hydrogel completed transformation from gel to sol (Figure 5A). However, the change of fluorescence intensity of TPE-Q19 sol was not observed (Figure 5B), indicating that the nanofiber structure still existed. So, the morphology of TPE-Q19 sol was examined by TEM. As shown in Figure 5C, nanofibers still existed after trypsin treatment, which might explain why the FL intensity didn't change. Although nanofibers were observed, they were fractured and did not show a closely entangled fibrous network as seen in the hydrogel (Figure 4C), which might explain why the gel converted to sol. Through

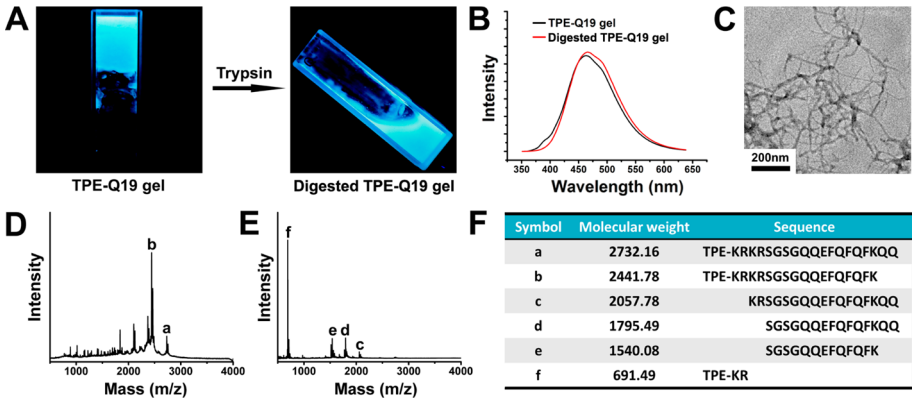

Symbol	Molecular weight	Sequence
a	2732.16	TPE-KRKRSGSGQQEFQFQFKQQ
b	2441.78	TPE-KRKRSGSGQQEFQFQFK
c	2057.78	KRSGSGQQEFQFQFKQQ
d	1795.49	SGSGQQEFQFQFKQQ
e	1540.08	SGSGQQEFQFQFK
f	691.49	TPE-KR

Figure 5. (A) Fluorescence images of the conversion from gel to sol of TPE-Q19 hydrogel (0.5 wt %) incubated with 0.025% trypsin for 12 h under a 365 nm UV lamp. (B) Fluorescence spectra of gel and sol of TPE-Q19 (0.5 wt %) incubated with 0.025% trypsin for 12 h (λ_{ex} = 330 nm). (C) Transmission electron microscopy (TEM) image of digested TPE-Q19 gel at 0.5 wt % concentration. (D) Sequence analysis of 0.025% trypsin treated TPE-Q19 hydrogel (0.5 wt %) and (E) TPE-Q19 solution (100 μM, 0.027 wt %) by MALDI-TOF-MS. (F) Table list of hydrolytic fragments of the trypsin treated TPE-Q19 hydrogel (0.5 wt %) and TPE-Q19 solution (100 μM, 0.027 wt %).

dx.doi.org/10.1021/am4049354 | ACS Appl. Mater. Interfaces 2014, 6, 757−762

determining the peptide segments of trypsin digested TPE-Q19 gel and TPE-Q19 water solution (100 μM, 0.027 wt %) (Figure 5D−F), we found that only two glutamines on the C-terminal were hydrolyzed in digested TPE-Q19 gel, whereas several segments were found in TPE-Q19 solution, especially the TPE-RK segment on the N-terminal. These results might provide us another evidence to confirm that TPE molecules were sequestered in the interior of the nanofibers and they were protected from the trypsin without being hydrolyzed.

CONCLUSIONS

In summary, we reported on the first example of conjugating TPE to salt-responsive peptide Q19 to form a luminescent hydrogel with enhanced emission. Our strategy can be applied to many traditional π-conjugated luminescent gelators suffering from the aggregation-caused quenching (ACQ) effect. Furthermore, the incorporation of Q11 section made the gel formation easily controllable and the gelation condition was mild which would be critical for tissue engineering and biosensing. We believed that the strategy described in this study would offer a general approach to control the emission of hydrogels. We are now seeking to conjugate AIE molecules to different stimuli-responsive peptides to explore the applications of luminescent hydrogels.

EXPERIMENTAL SECTION

Preparation of the Luminescent Hydrogel. Five milligrams of TPE-Q19 was dissolved in 1.0 mL of water, and NaCl solutions of a concentration gradient were added into the peptide solution. When the NaCl concentration increased to 1.0 M, hydrogel formed immediately. It was unadvisable to dissolve the peptide into the NaCl solution directly, which would lead to the precipitate of the peptide.

ASSOCIATED CONTENT

Supporting Information

Materials, general methods, synthesis and characterization of TPE-COOH and peptides, emission spectra, and TEM images. This material is available free of charge via the Internet at http://pubs.acs.org.

AUTHOR INFORMATION

Corresponding Authors

*E-mail: zougz@nanoctr.cn. Fax: +86-010-62656765. Tel: +86-010-82545530.

*E-mail: liangxj@nanoctr.cn.

Author Contributions

‡Authors C.Z. and C.L. contributed equally to this report.

Notes

The authors declare no competing financial interest.

ACKNOWLEDGMENTS

This work was financially supported in part by grants from the State High-Tech Development Plan (2012AA020804), National Natural Science Foundation of China (30970784, 31170873, and 81171455), National Key Basic Research Program of China (2009CB930200), National Distinguished Young Scholars grant (31225009), National Natural Science Foundation of China, and Chinese Academy of Sciences (CAS) "Hundred Talents Program" (07165111ZX).

REFERENCES

(1) Wang, H.; Wei, J.; Yang, C.; Zhao, H.; Li, D.; Yin, Z.; Yang, Z. *Biomaterials* **2012**, *33*, 5848−5953.
(2) Pan, Y.; Du, X.; Zhao, F.; Xu, B. *Chem. Soc. Rev.* **2012**, *41*, 2912−2942.
(3) Komatsu, H.; Matsumoto, S.; Tamaru, S.; Kaneko, K.; Ikeda, M.; Hamachi, I. *J. Am. Chem. Soc.* **2009**, *131*, 5580−5585.
(4) Xu, X. D.; Liang, L.; Chen, C. S.; Lu, B.; Wang, N. L.; Jiang, F. G.; Zhang, X. Z.; Zhuo, R. X. *ACS Appl. Mater. Interfaces* **2010**, *2*, 2663−2671.
(5) Rudra, J. S.; Tian, Y. F.; Jung, J. P.; Collier, J. H. *Proc. Natl. Acad. Sci. U.S.A.* **2010**, *107*, 622−627.
(6) Jung, J. P.; Nagaraj, A. K.; Fox, E. K.; Rudra, J. S.; Devgun, J. M.; Collier, J. H. *Biomaterials* **2009**, *30*, 2400−2410.
(7) Panda, J. J.; Dua, R.; Mishra, A.; Mittra, B.; Chauhan, V. S. *ACS Appl. Mater. Interfaces* **2010**, *2*, 2839−2848.
(8) Maude, S.; Ingham, E.; Aggeli, A. *Nanomedicine* **2013**, *8*, 823−847.
(9) Kyle, S.; Felton, S. H.; McPherson, M. J.; Aggeli, A.; Ingham, E. *Adv. Healthcare Mater.* **2012**, *1*, 640−645.
(10) Bremmer, S. C.; Chen, J.; McNeil, A. J.; Soellner, M. B. *Chem. Commun.* **2012**, *48*, 5482−5484.
(11) Bhuniya, S.; Kim, B. H. *Chem. Commun.* **2006**, 1842−1844.
(12) Heo, Y. J.; Shibata, H.; Okitsu, T.; Kawanishi, T.; Takeuchi, S. *Proc. Natl. Acad. Sci. U.S.A.* **2011**, *108*, 13399−13403.
(13) Kim, J. H.; Lim, S. Y.; Nam, D. H.; Ryu, J.; Ku, S. H.; Park, C. B. *Biosens. Bioelectron.* **2011**, *26*, 1860−1865.
(14) Luo, J.; Xie, Z.; Lam, J. W.; Cheng, L.; Chen, H.; Qiu, C.; Kwok, H. S.; Zhan, X.; Liu, Y.; Zhu, D.; Tang, B. Z. *Chem. Commun.* **2001**, 1740−1741.
(15) Wang, J.; Mei, J.; Hu, R.; Sun, J. Z.; Qin, A.; Tang, B. Z. *J. Am. Chem. Soc.* **2012**, *134*, 9956−9966.
(16) Hong, Y.; Meng, L.; Chen, S.; Leung, C. W.; Da, L. T.; Faisal, M.; Silva, D. A.; Liu, J.; Lam, J. W.; Huang, X.; Tang, B. Z. *J. Am. Chem. Soc.* **2012**, *134*, 1680−1689.
(17) Du, X. B.; Qi, J.; Zhang, Z. Q.; Ma, D. G.; Wang, Z. Y. *Chem. Mater.* **2012**, *24*, 2178−2185.
(18) Shustova, N. B.; Ong, T.-C.; Cozzolino, A. F.; Michaelis, V. K.; Griffin, R. G.; Dinca, M. *J. Am. Chem. Soc.* **2012**, *134*, 15061−15070.
(19) Kapadia, P. P.; Ditzler, L. R.; Baltrusaitis, J.; Swenson, D. C.; Tivanski, A. V.; Pigge, F. C. *J. Am. Chem. Soc.* **2011**, *133*, 8490−8493.
(20) Xu, B.; Chi, Z.; Li, H.; Zhang, X.; Li, X.; Liu, S.; Zhang, Y.; Xu, J. *J. Phys. Chem. C* **2011**, *115*, 17574−17581.
(21) Huang, X.; Gu, X.; Zhang, G.; Zhang, D. *Chem. Commun.* **2012**, *48*, 12195−12197.
(22) Xu, X.; Li, J.; Li, Q.; Huang, J.; Dong, Y.; Hong, Y.; Yan, J.; Qin, J.; Li, Z.; Tang, B. Z. *Chemistry - Eur. J.* **2012**, *18*, 7278−7286.
(23) Li, C.; Wu, T.; Hong, C.; Zhang, G.; Liu, S. *Angew. Chem., Int. Ed.* **2012**, *51*, 455−459.
(24) Zhao, Z.; Lam, J. W.; Chan, C. Y.; Chen, S.; Liu, J.; Lu, P.; Rodriguez, M.; Maldonado, J. L.; Ramos-Ortiz, G.; Sung, H. H.; Williams, I. D.; Su, H.; Wong, K. S.; Ma, Y.; Kwok, H. S.; Qiu, H.; Tang, B. Z. *Adv. Mater.* **2011**, *23*, 5430−5435.
(25) Collier, J. H.; Messersmith, P. B. *Bioconjugate Chem.* **2003**, *14*, 748−755.
(26) Jung, J. P.; Nagaraj, A. K.; Fox, E. K.; Rudra, J. S.; Devgun, J. M.; Collier, J. H. *Biomaterials* **2009**, *30*, 2400−2410.
(27) Collier, J. H. *Soft Matter* **2008**, *4*, 2310−2315.
(28) Jung, J. P.; Jones, J. L.; Cronier, S. A.; Collier, J. H. *Biomaterials* **2008**, *29*, 2143−2151.
(29) Aggeli, A.; Bell, M.; Boden, N.; Keen, J. N.; Knowles, P. F.; McLeish, T. C.; Pitkeathly, M.; Radford, S. E. *Nature* **1997**, *386*, 259−262.
(30) Holmes, T. C.; de Lacalle, S.; Su, X.; Liu, G.; Rich, A.; Zhang, S. *Proc. Natl. Acad. Sci. U. S. A.* **2000**, *97*, 6728−6733.
(31) Gras, S. L.; Tickler, A. K.; Squires, A. M.; Devlin, G. L.; Horton, M. A.; Dobson, C. M.; MacPhee, C. E. *Biomaterials* **2008**, *29*, 1553−1562.

(32) Schneider, J. P.; Pochan, D. J.; Ozbas, B.; Rajagopal, K.; Pakstis, L.; Kretsinger, J. *J. Am. Chem. Soc.* **2002**, *124*, 15030−15037.
(33) Haines, L. A.; Rajagopal, K.; Ozbas, B.; Salick, D. A.; Pochan, D. J.; Schneider, J. P. *J. Am. Chem. Soc.* **2005**, *127*, 17025−17029.
(34) Hartgerink, J. D.; Beniash, E.; Stupp, S. I. *Science* **2001**, *294*, 1684−1688.
(35) ysseling-Mattiace, V. M.; Sahni, V.; Niece, K. L.; Birch, D.; Czeisler, C.; Fehlings, M. G.; Stupp, S. I.; Kessler, J. A. *J. Neurosci.* **2008**, *28*, 3814−3823.
(36) Zhang, S.; Greenfield, M. A.; Mata, A.; Palmer, L. C.; Bitton, R.; Mantei, J. R.; Aparicio, C.; de la Cruz, M. O.; Stupp, S. I. *Nat. Mater.* **2010**, *9*, 594−601.
(37) Zhou, M.; Smith, A. M.; Das, A. K.; Hodson, N. W.; Collins, R. F.; Ulijn, R. V.; Gough, J. E. *Biomaterials* **2009**, *30*, 2523−2530.
(38) Rudra, J. S.; Tian, Y. F.; Jung, J. P.; Collier, J. H. *Proc. Natl. Acad. Sci. U.S.A.* **2010**, *107*, 622−627.
(39) Collier, J. H.; Hu, B. H.; Ruberti, J. W.; Zhang, J.; Shum, P.; Thompson, D. H. *J. Am. Chem. Soc.* **2001**, *123*, 9463−9464.
(40) Lee, N. R.; Bowerman, C. J.; Nilsson, B. L. *Biomacromolecules* **2013**, *14*, 3267−3277.
(41) Biancalana, M.; Koide, S. *Biochim. Biophys. Acta* **2010**, *1804*, 1405−1412.